








Received:  
September 30, 2022

Accepted:  
October 27, 2022

Published:  
October 31, 2022

## Evaluation of Non-Newtonian Fluid Flow in Coiled Tubing

Lorena Rodrigues Justino<sup>1</sup> , Beatriz Rosas de Oliveira<sup>1</sup> , José Marcelo Silva Rocha<sup>2</sup> , Rodrigo Fernando de Oliveira Borges<sup>3</sup> , Cristiano Agenor Oliveira de Araújo<sup>4</sup> , Cláudia Miriam Scheid<sup>1</sup> , Luís Américo Calçada<sup>1</sup> 

<sup>1</sup> Federal Rural University of Rio de Janeiro, Seropédica, Brazil.

<sup>2</sup> Petróleo Brasileiro SA PETROBRAS, Rio de Janeiro, RJ, Brazil.

<sup>3</sup> AP Consultoria e Projetos, Salvador, Brazil.

<sup>4</sup> Federal University of Jequitinhonha and Mucuri Valleys, Teófilo Otoni, Brazil.

### Email address

lorisjustino@gmail.com (Lorena R. Justino)

oliveira.biarosas@gmail.com (Beatriz R. Oliveira)

jmrocha@petrobras.com.br (José M. S. Rocha)

rfernando.rfob@gmail.com (Rodrigo F. O. Borges)

cristianoagenor@ufvjm.edu.br (Cristiano A. O. Araújo) – Corresponding author.

scheid@ufrj.br (Cláudia M. Scheid)

calcada@ufrj.br (Luís A. Calçada)

### Abstract

The coiled tubing system is made up of a long and flexible steel tube wound around a coil, which can reach over 6000 meters in length. During operation, part of the tube remains wound on the spool, while the other part is directed into the well. In this tube, different types of fluids, such as water, cement paste and displacement fluid, are pumped in order to ensure the isolation of the well. This work presents three stage of experiment that was carried out with water and xanthan gum solutions that had rheological properties and behavior that approximated a used cement paste. In the first stage of this study, data from pumping water and cement paste in a real well abandonment process were used to validate a mathematical modeling. The simulated data approximated the field data with a mean relative error below 9%. In the second stage experiments were carried out with xanthan gum solution at a concentration of 0.5 lb bbl<sup>-1</sup>, and temperatures of 30°C and 40°C. The objective of this study was to verify if the model proposed by the author is valid for different concentrations and temperatures. Finally, in the third stage of the study, simulations were carried out in order to obtain the maximum pumping capacity of the system, with the installation of a new pump. The simulated data shown that the water flow reached the turbulent regime with a maximum pumping flow of 2 m<sup>3</sup> h<sup>-1</sup>, while the flow of the xanthan gum solution did not reach the turbulent regime, even reaching a maximum flow of 3 m<sup>3</sup> h<sup>-1</sup>.

**Keywords:** Coiled tubing, Pressure drop, Well abandonment.

## 1. Introduction

Coiled tubing is a very long flexible steel tube wound around a coil, which can reach over 6000 meters in length. During operation, part of the tube remains wound on the spool, while the other part is directed into the well. In this tube, different types of fluids, such as water, cement paste and displacement fluid, are pumped in order to ensure the isolation of the well. Used in various industrial applications, the coiled tubing system

has grown significantly over the years. According to Bracamonte and Diaz, (2018), the use of coiled tubing systems between 2002 and 2017 doubled, and this reveals how much their usefulness has been growing, especially in the oil area (ICOTA, 2019). In addition, the equipment has wide applicability both in exploration and in well construction, mainly used in drilling, well completion, well cleaning and abandonment, acidification and maintenance processes (Jain, Singhal and Shah, 2004).

In order to compare with a straight pipe system, such as the use of drill pipes, the coiled tubing system has a significant advantage consisting in the reduction of operating time due to its continuous structure, without the need to connect and disconnect the pipes (Oliveira *et al.*, 2021). Because of this, the curved pipe system is also capable of reducing the costs of the process, and ends up becoming a more viable option in the operation.

The pressure drop in a curved tube is significantly greater than the pressure drop in straight tubes, especially in the flow of non-Newtonian fluids such as cement paste. Several authors have developed experimental studies that justify the significant difference between the flow of the same fluid in a straight tube and in a curved tube (White, 1929; Azouz *et al.*, 1998; Jain, Singhal and Shah, 2004; Zhou and Shah, 2004; Cioncolini and Santini, 2006).

One of the most important concepts to consider in helical tubes is the curvature ratio. The concept of the curvature ratio was first defined by Dean, (1927), being the ratio between the inner radius of the tube ( $r$ ) and the curvature radius ( $R$ ) in which the tube is wound. According to Medjani and Shah, (2000) the curvature ratio can be defined as a function of the number of layers in the tube. Thus, the coiled tubing system has numerous layers, so the equation (Equation 1) most suitable for calculating the radius of curvature is the one cited by the authors

$$\frac{r}{R} = \frac{r}{R_c + (2 \cdot N - 1)r} \quad (1)$$

where  $r$  is the inner radius of the tube,  $R$  is the radius of curvature,  $R_c$  is the reel radius, and  $N$  is the number of layer.

The Dean number ( $De$ ) is a very relevant dimensionless, mainly in the flow of fluids in curved pipes. It plays a key role in friction factor correlations, in addition to being used to characterize the axial velocity profile. Therefore, the dimensionless one considers the effect of inertial, centrifugal and viscous forces, demonstrated by Equation 2, proposed by White, (1929), which is the most applied equation in the study of the flow of curved pipes by several authors (Zhou and Shah, 2004; Shaqlaih and Ahmed Kamel, 2013)

$$De = Re \sqrt{\frac{r}{R}}, \quad (2)$$

where  $De$  is the Dean number,  $Re$  the Reynolds number,  $r$  the inner radius of the pipe and  $R$  the curvature radius.

The Reynolds number is an important dimensionless and is directly associated to the type of flow regime of a fluid. Equation 3 shows how the Reynolds number is calculated for non-Newtonian fluids that follow the Power-law model (Rep)

$$Re_p = \frac{D \langle v \rangle \rho}{k \left( \frac{8v}{D} \right)^{n-1} \left( \frac{3n+1}{4n} \right)^n} \quad (3)$$

where  $D$  is the tube diameter (m),  $\langle v \rangle$  is the average fluid velocity ( $m \cdot s^{-1}$ ),  $\rho$  is the fluid density ( $kg \cdot m^{-3}$ ),  $K$  is the consistency index of Power Law rheological model ( $Pa \cdot s^n$ ),  $n$  is the flow index of Power Law rheological model (dimensionless).

Another important dimensionless parameter to be evaluated in the flow in curved pipes is the friction factor ( $f_c$ ), which aims to calculate the pressure loss (or head loss) due to friction, that considers the effect of resistance in the flow of a fluid with the pipe walls (frictions loss) and pipe fittings (local loss). Some authors have developed friction factor correlations experimentally, analytically or numerically, both for straight and curved tubes. According to the work of Zhou and Shah, (2004), proposals for the prediction of friction factors for Newtonian fluids in laminar regime of curved pipes can be found in the works of Mishra and Gupta (1979), Srinivasan, Nandapurkar and Holland, (1970), Ito (1959), White (1932), among others. For the turbulent regime, the friction factor equations gained prominence in the works of Mishra and Gupta (1979), Srinivasan, Nandapurkar and Holland (1970) and Ito (1959). For non-Newtonian fluids in laminar and turbulent regimes, correlations for the friction factor can be found in the works of Mashelkar and Devarajan, (1977), Mishra and Gupta (1979), McCann and Islas (1996) and Willingham and Shah (2000).

Oliveira *et al.* (2021) proposed a mathematical modeling (Equation 4) to simulate the pressure drop in the flow of a sequence of fluids in a coiled tubing with field data, in order to develop a simulator to be applied in the oil industry. The purpose of developing this methodology was to simulate not only

experimental data, but also real cases of oil well abandonment.

$$f_c = \frac{16}{Re_p} [0,73 + 0,0057(\log. De)^{4,92}] \quad (4)$$

The mathematical modeling proposed by Oliveira *et al.* (2021) was used to calculate the head loss of a real well abandonment process. The differential of this new modeling was the variation of the internal pipe diameter along its length, in addition of pumping a sequence of fluids. As different fluids with different flow rates are pumped in sequence in a real case, a head loss profile is obtained as a function of process time.

As the position of the fluids varies along the length of the coiled tubing as a function of time, it is necessary to identify the interface between them. When calculating the pressure drop in each layer, it is necessary to consider the length occupied by each fluid and, consequently, its physical properties. The resolution of the mathematical modeling was done in FORTRAN language, and the input data were: the fluid pumping sequence (flow rate and pumping time), the properties of each fluid (rheological parameters and density) and the coiled tubing geometry (radius and width of reel, outer pipe radius, number of sections with different internal diameters, length and inner radius of each section and length of pipe inside the well). As output data, the total pressure drop is available in each layer as a function of time.

The aim of this work was, in the first stage of this study, data from pumping water and cement paste in a real well abandonment process were used to validate the mathematical modeling proposed by Oliveira *et al.* (2021). In the second stage, to evaluate the mathematical modeling proposed by Oliveira *et al.* (2021) at a different concentration from that used by the author (2 lb bbl<sup>-1</sup>), experiments were carried out with xanthan gum solution at a concentration of 0.5 lb bbl<sup>-1</sup>, and temperatures of 30°C and 40°C. The objective of this study was to verify if the model proposed by the author is valid for different concentrations and temperatures. In the third stage of the study, simulations were carried out in order to obtain the maximum pumping capacity of the system, with the installation of a new pump.

## 2. Materials and Methods

### 2.1. Experimental rig

The experimental rig used in this work to calculate the pressure drop in the flow of water and xanthan gum is represented by the schematic drawing in Figure (1).

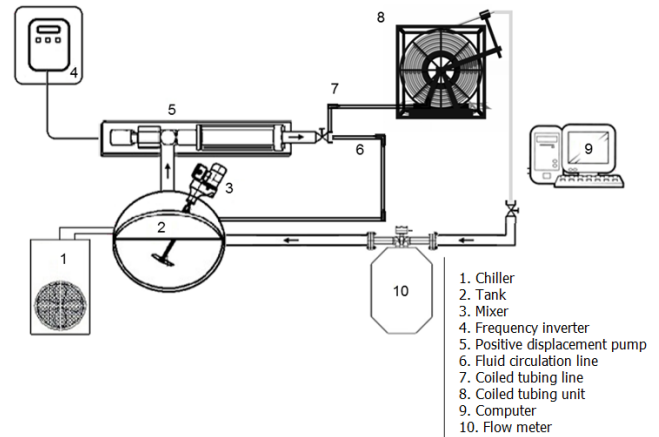


Figure 1 – Schematic drawing of the experimental rig and equipments (Adapted from Pereira, 2018).

The fluid was prepared in a jacketed tank [2], which also has an agitator [3] helping to mix the fluid. The fluid temperature is controlled by three internal resistors in the tank, as well as by the chiller [1]. By controlling the temperature of the fluid, the flow is started through a positive displacement pump [5]. Both pump rotation and fluid flow are controlled by means of a frequency inverter [4]. The fluid circulation line [6] integrates a 2 in steel pipe that leads the fluid to the coiled tubing unit [8] where it has pressure and temperature gauges in each layer. Before returning to the tank, the fluid passes through a flow meter [10] where the pumping circuit ends.

This unit contains a copper coil, Figure (2), which simulates coiled tubing. It has eight layers and, consequently, eight curvature ratios ranging from 0.014 to 0.018. Each layer consists of twenty turns, totaling 375.8 m. The coil has an inner diameter (Dint) of 61.5 cm and an outer diameter (Dext) of 79.1 cm. The tube has a diameter (Dtube) of 1.11 cm.

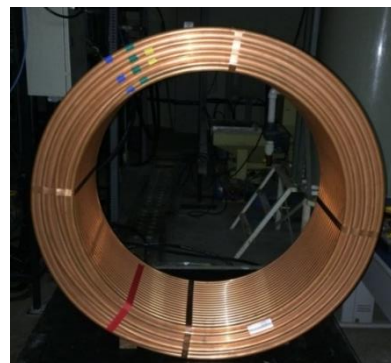


Figure 2 – Image of the copper coil representing the coiled tubing in the pilot unit.

To obtain the pressure and temperature values in the fluids pumped in the coiled tubing unit, gauge pressure transmitters and thermocouples, Figure (3), were installed in each layer.

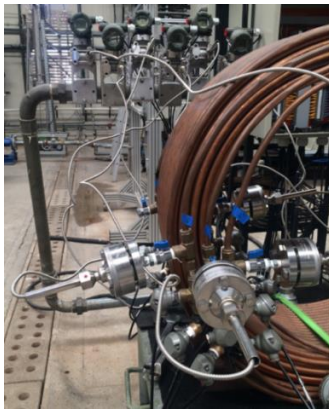


Figure 3 – Gauge pressure and temperature transmitters installed in the coiled tubing unit.

## 2.2. Case Study

The methodology proposed by Oliveira et al. (2021) to calculate the head loss in fluid flow in a coiled tubing system, aims to simulate not only the experimental data obtained in the laboratory, but also the field data in a real case in a process of abandonment of well. Therefore, field data were provided by the Leopoldo Américo Miguez de Mello Research Center (CENPES). The simulation of these data was performed in the FORTRAN language. By running the program, it was possible to obtain the results of pressure drop in each layer as a function of time.

In order to evaluate the simulation, the Percentage Relative Error (PRE) (Equation 5) was calculated using the experimental (Exp.) and calculated (Calc.) values of pressure drop.

$$PRE(\%) = \frac{|Exp. value - Calc. value|}{Exp. value} \times 100 \quad (5)$$

## 2.3. Characterization of the xanthan gum solution

To evaluate the pressure drop in non-Newtonian fluids in curved tubes, the xanthan gum solution was chosen, due to the rheological similarity with the cement slurries. Therefore, a series of experiments were carried out using the xanthan gum solution at a concentration of 0.5 lb bbl-1 (1.43 kg m-3), at temperatures of 30°C and 40°C.

To perform the rheological analysis of the xanthan gum solution, the Fann viscometer (Model

35A), Figure (4), was used at rotations of 0.9, 1.8, 3, 6, 30, 60, 90, 100, 180, 200, 300 and 600, where the shear rates, which is a function of rotation, are equivalent to 1.5, 3.1, 5.1, 10.2, 51.1, 102, 153, 170, 306, 340, 511, and 1021, respectively.



Figure 4 – Fann Viscometer model 35A (Fann Instruments).

For each rotation, a shear is applied to the fluid, where the deformation occurs, being possible to quantify the shear stress. Readings were taken in ascending order. Based on the rotations and reading angles in the viscometer, the values of shear stress ( $\tau$ ) and shear rate ( $\lambda$ ) were calculated. The calculation was performed using equations (6) and (7), related to the R1 B1 set (Rotor-Bob Combinations) of the viscometer

$$\tau = 0,511 \times \theta , \quad (6)$$

$$\lambda = 1,7023 \times rpm , \quad (7)$$

where  $\theta$  is the deformation angle read on the equipment ( $^{\circ}$ ) and rpm is the rotations per minute of the viscosimeter.

The Power-Law model, Equation 8, was used to describe the behavior of xanthan gum solution. This model was chosen because most of the friction factor correlations, for non-Newtonian flows in coiled tubing, found in the literature, are based on this model

$$\tau = k\lambda^n , \quad (8)$$

where k is the consistency index (Pa sn) and n is the flow index (dimensionless).

The values of the rheological parameters k and n can be obtained through the linearization of equation (8), which involves the stress and strain rate data. The linearized equation is:

$$\ln \tau = n \ln \lambda + \ln k \tag{9}$$

The mean values of n and k for three samples were obtained experimentally for xanthan gum solutions (Table 1) with a concentration of 0.5 lb/bbl (1.43 kg/m<sup>3</sup>).

Table 1 – Mean values of n and k for xanthan gum solutions with a concentration of 0.5 lb/bbl.

Parameter	Value	T(°C)	δ	S <sup>2</sup>
n	0.4856	30	7.78E-03	6.06E-05
n	0.5051	40	2.2E-02	4.98E-04
k	0.3049	30	1.78E-03	3.17E-06
k	0.1618	40	5.1E-02	2.61E-03

Where, T is the temperature, δ is the standard deviation and S<sup>2</sup> is the variance.

The density of the xanthan gum solution was obtained using the Fann model 140 mud balance, shown in Figure (5). The density of the xanthan gum was 991 kg m<sup>-3</sup>.

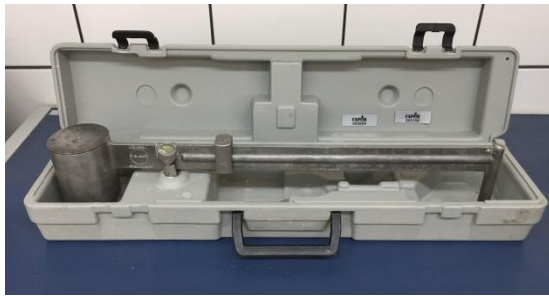


Figure 5 - Fann model 140 mud balance.

#### 2.4. Simulation of experimental data in xanthan gum solution with a concentration of 0.5 lb bbl<sup>-1</sup>

In this stage, new experiments were carried out in the coiled tubing unit to obtain the pressure drop in a non-Newtonian fluid, composed of a xanthan gum solution, 0.5 lb bbl<sup>-1</sup> (1.43 kg/m<sup>3</sup>), at temperatures of 30°C and 40°C, in each layer, in order to verify if the mathematical modeling proposed by Oliveira et al. (2021), that works with xanthan gum solution with 2 lb bbl<sup>-1</sup>, is able to preview these values in this range of concentration.

Different curvature ratios and volumetric flow rates were used in these experiments to obtain the pressure drop. The xanthan gum solution was pumped in the coiled tubing system with flow rates of 0.25, 0.50, 0.75, 1.0, 1.25 and 1.50 m<sup>3</sup> h<sup>-1</sup>. To reduce the heat transfer with the environment, the coil was thermally insulated with a ceramic fiber tape (Figure 6).



Figure 6 – Thermally insulated coil with ceramic fiber tape.

The xanthan gum solution was prepared with 0.5 lb bbl<sup>-1</sup>, 1.25% v/v defoamer, and 0.125% v/v bactericide (glutaraldehyde). The experimental data were obtained in triplicate, and the values were compared with the modeling proposed by Oliveira et al. (2021). The friction factor correlation for xanthan gum solution (fcg) proposed by Oliveira et al. (2021) (Equation 4) was used and the pressure drop calculation was performed using Equations 10 and 11

$$\Delta P_{TOTAL} = \Delta P_{1^{a} layer} + \Delta P_{2^{a} layer} + \dots + \Delta P_{n-layer} \tag{10}$$

$$\left(\frac{\Delta P}{\rho g}\right) = \left(2f_1 \frac{L_1 v^2}{D g}\right)_{1^{a} layer} + \left(2f_2 \frac{L_2 v^2}{D g}\right)_{2^{a} layer} + \dots + \left(2f_n \frac{L_n v^2}{D g}\right)_{n-layer} \tag{11}$$

where, D is the inner diameter of the tube, v is the average velocity of the fluid, ρ is the density of the fluid and L is the length of the tube.

In this experiment, the layer-to-layer pressure difference can be obtained. By Equation 12, the total pressure drop of the coiled tubing is given by the sum of the pressure drop layer by layer.

The experimentally mean values of n and k of three were obtained for xanthan gum solutions with a concentration of 0.5 lb bbl<sup>-1</sup>, was shown in Table (1).

#### 2.5. Simulation of the maximum operating flow of the new pump

The purpose of a new pump in the experimental unit was to achieve higher flow rates and, consequently, higher Reynolds (Re) ranges. For this, the discharge pressure of the new pump was considered. Water was pumped into the experimental unit at a temperature of 25°C. The xanthan gum solution was pumped into the system

at a concentration of 2 lb/bbl (5.71 kg m<sup>-3</sup>) in 150 L of water, at a temperature of 40°C. Therefore, 5% v/v of defoamer was added to the formulation, in order to reduce the generation of bubbles and foams, and 0.5% v/v of bactericide (glutaraldehyde), in which the function was to prevent deterioration of the polymer.

Table 2 - Presents the specifications of the new pump attached to the pilot unit.

Pump Specification	
Operation temperature (°C)	25 a 70
Project flow rate (m <sup>3</sup> h <sup>-1</sup> )	7.8
Nominal flow rate (m <sup>3</sup> h <sup>-1</sup> )	7.9
Discharge pressure (Pa)	1.2E+06
Rotation (rad s <sup>-1</sup> )	28.17
Absorbed power (W)	2.70E+03
Motor power (w)	5.60E+03

To obtain the maximum pumping capacity of the unit, the following parameters were used to calculate the pressure drop: the curvature ratio (r/R) (Equation 1), the Reynolds number of non-Newtonian fluid described by Power-Law rheological model (ReP) (Equation 3), the Dean number (De) (Equation 2), the friction factor of xanthan gum (fcg) (Equation 4), the friction factor of water (fca), and the pressure drop equation in a layer (ΔP), represented by Equations 12 and 13

$$f_{ca} = \frac{1}{4} \left(\frac{r}{R}\right)^{0,5} \left\{ 0,029 + 0,304 \left[ \text{Rep} \left(\frac{r}{R}\right)^2 \right]^{-0,25} \right\} \quad (12)$$

$$\Delta P = \frac{2 \cdot \rho \cdot f \cdot L \cdot v^2}{R_{int} \cdot 2} \quad (13)$$

where R<sub>int</sub> is the inner radius of the tube, R is the curvature radius, v is the average velocity of the fluid, ρ is the density of the fluid, and L is the length of the tube. The total pressure drop of the unit was obtained by summing the head loss in each layer.

### 3. Results and discussion

#### 3.1. Case study (field data)

The case study data were obtained from a well abandonment process in the Campos Basin with pumping water and cement paste provided by the Leopoldo Américo Miguez de Mello Research Center (CENPES). The coiled tubing used in the

process consisted of 12 layers and 3 internal diameters, totaling 3300 meters of coiled tube. With this data, through the mathematical modeling proposed by Oliveira et al. (2021), it was possible to evaluate field and experimental data in order to predict whether the modeling proposed by the author is effective.

Table (3) shows the geometry of the coiled tubing, in which the total length of the tube is divided into three sections with three different internal diameters.

Table 3 – Coiled tubing geometry data of Campos basin.

Section number	Length (m)	Inner diameter (m)
1	1056.7	0.0284
2	1310.6	0.0292
3	943.9	0.0302

Table (4) presents the pumping data of the process whose total operating time was 34 minutes.

Table 4 – Operational data from the case study.

Fluid	Time of pumping (min)	Flow rate (bbl min <sup>-1</sup> )
Water 1	12	0.7
Cement paste	5	0.75
Cement paste	4	0.6
Cement paste	9	0.85
Water 2	4	0.75

Table (5) presents the properties of the pumped fluids (density and rheological parameters of the Power-Law model).

Table 5 – Data of the fluid properties pumped on the case study.

Fluid	ρ <sub>r</sub> (kg m <sup>-3</sup> )	n (dimens-less)	k (Pa s)
Water 1	1000	1	0.0011
Cement paste	1893	0.75	0.28
Cement paste	1893	0.75	0.28
Cement paste	1893	0.43	0.69
Water 2	1000	1	0.0011

Figure (7) shows the total pressure drop as a function of process time for pumping water and cement paste. The black line represents simulated data and symbols represent experimental data. The numbers contained in the symbol legend refer to the fluid pumping order.

It is possible to observe that the proposed simulator was able to predict with a good accuracy (in some situations) the pressure drop in the fluid

flow in coiled tubing of a real process. It is important to emphasize that the variation of the curvature ratio in each layer, the variation of the internal diameter in the length of the tube and the pumping of a sequence of fluids were considered.

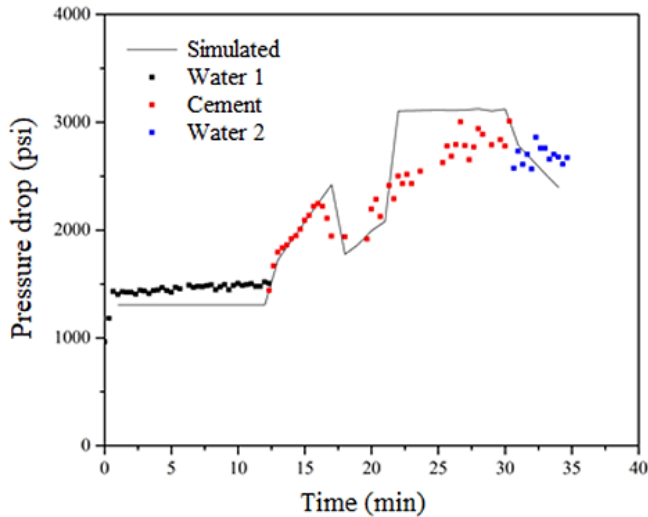


Figure 7 – Total pressure drop as a function of time in pumping water and cement paste (case study).

In the first few minutes of the process, the total pressure drop remains constant, as only water is being pumped. However, at 12 minutes into the process, the cement paste starts to be pumped and the total pressure drop increases linearly with time. This is because as the cement is pumped in the system, water is being withdrawn and the cement provides a higher pressure drop when flowing. At 17 minutes, the cement flow rate increased and, consequently, the total pressure drop increased. At 21 minutes, the cement pressure drop remained constant. It can be seen that in this region the experimental points are far from the curve of the simulated data, which makes some adjustments necessary. In the last cement pumping, there was an increase in flow and all water was removed from the system, so the total pressure loss became constant. In the last water pumping, there was a drop in the total head loss, as water offers a lower pressure drop compared to cement paste.

Table (6) presents the relative error of each pumping stage, with their respective volumetric flows and operating time. Taking into account an average across all steps, the simulator was able to predict the dynamic pressure profile of the field data with an absolute average relative error of 9%.

### 3.2. Comparison of experimental and simulated xanthan gum solution data

Table 6 – Absolute mean error in the calculation of the pressure drop for each pumping stage.

Fluid	Flow rate (bbl min <sup>-1</sup> )	Absolute mean error (%)
Water 1	0.7	10.4
Cement paste	0.75	5.5
Cement paste	0.6	8.5
Cement paste	0.85	14.5
Water 2	0.75	6.11

To evaluate the mathematical modeling proposed by Oliveira et al. (2021) at a concentration different from that used by the author (2 lb bbl-1), experiments were carried out with xanthan gum solution at a concentration of 0.5 lb bbl-1, and temperatures of 30°C and 40°C. The objective of this study was to verify if the model proposed by the author is valid for different concentrations and temperatures. The experimental data, obtained in triplicate, were compared with the model by Oliveira et al. (2021), implemented in a program with the FORTRAN programming language.

The graphs in Figures (8) and (9) show the pressure drop values by flow rate of experimental and calculated xanthan gum solution, in each layer at temperatures of 30°C and 40°C, respectively. Only four layers are presented, 1st, 3rd, 5th and 8th, due to the results of the others being similar.

It is possible to observe that at the temperature of 30°C, with the increase of the flow rate, and consequently, of the pressure drop, the percentage errors gradually decrease. The same behavior can be observed in the results obtained at 40°C.

However, it is possible to observe that at the temperature of 40°C the average percentage errors, 18.4%, are much smaller than the average percentage errors obtained at the temperature of 30°C, which was 37.8%. This can be explained by the friction factor correlation proposed by Oliveira et al. (2021) for the xanthan gum solution, having been developed at a temperature of 40°C and at a concentration of 2 lb bbl-1. Therefore, the objective is to be as comprehensive as possible, in order to increase the range of temperature, concentration and curvature ratio, so that the proposed friction factor correlation can achieve greater applicability. The data obtained at the temperature of 40°C adjusted better than at the temperature of 30°C, according to the average percentage errors presented. Therefore, it is necessary to reestimate the friction factor correlation parameters for these new solutions.

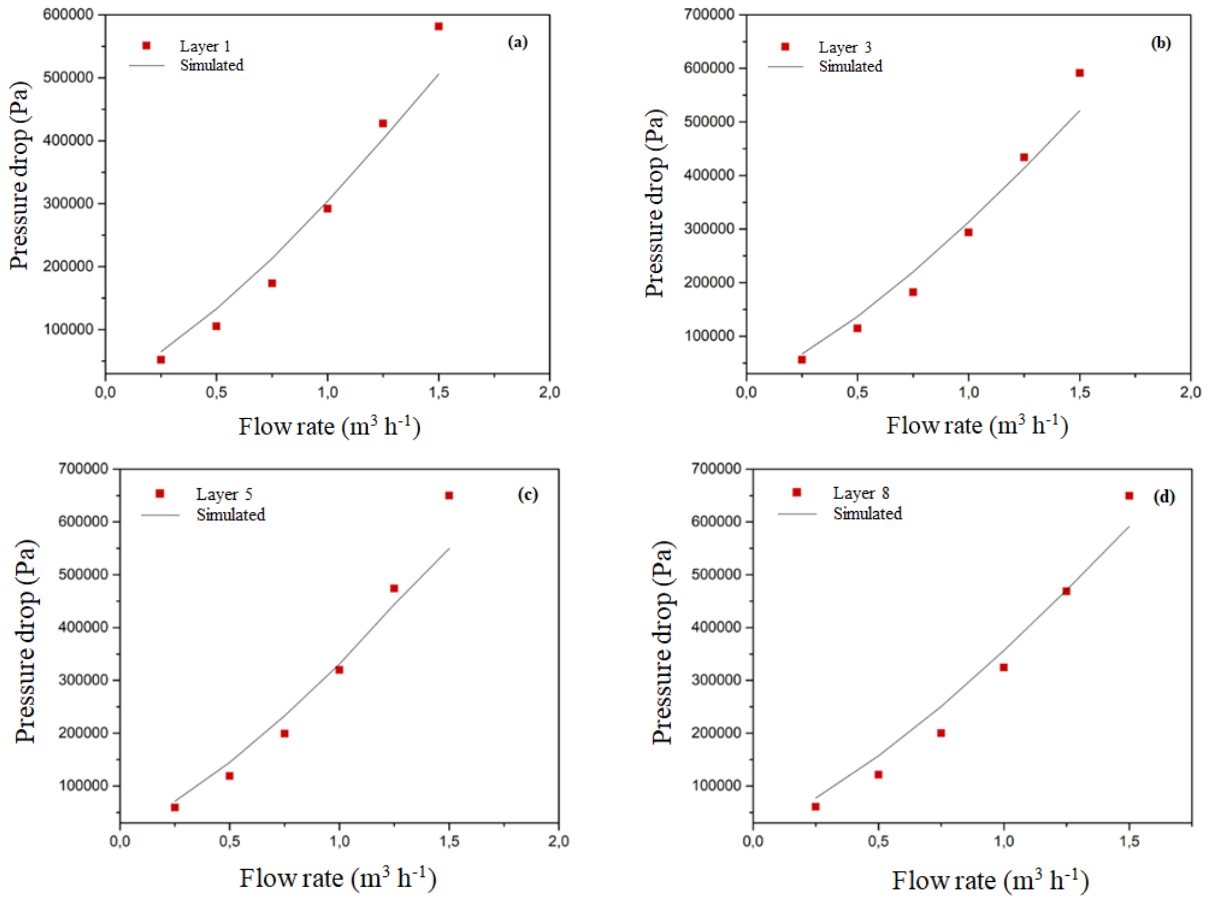


Figure 8 – Experimental and calculated pressure drop as a function of flow rate in xanthan gum solution for a) 1<sup>st</sup>, b) 3<sup>rd</sup>, c) 5<sup>th</sup> and d) 8<sup>th</sup> layer at a temperature of 30°C.

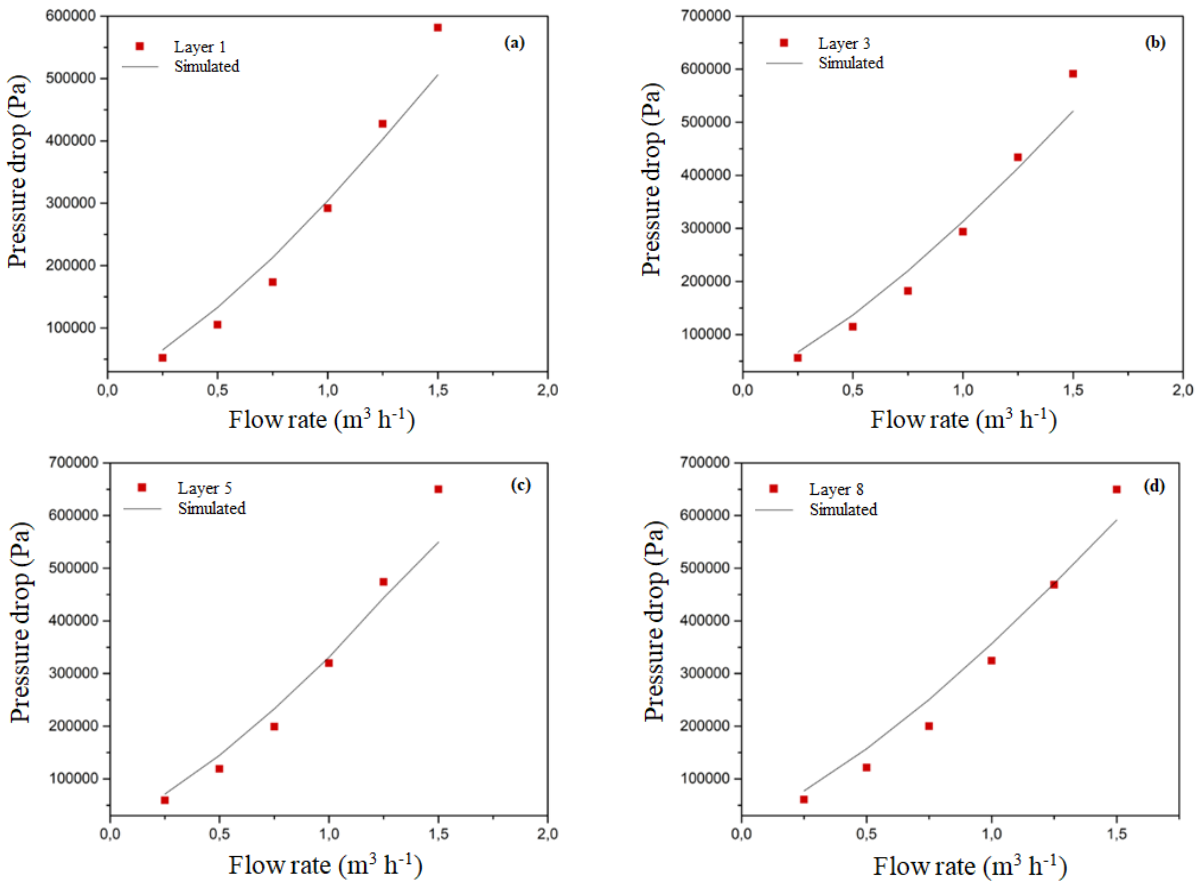


Figure 9 – Experimental and calculated pressure drop as a function of flow rate in xanthan gum solution for a) 1<sup>st</sup>, b) 3<sup>rd</sup>, c) 5<sup>th</sup> and d) 8<sup>th</sup> layer at a temperature of 40°C.



**3.3. Simulation of pressure drop in pilot unit with the new pump**

Through the experimental data obtained by Pereira (2018) for water, and the experimental data of xanthan gum obtained by Oliveira et al. (2021), it was possible to evaluate the pressure drop and the operating flow of the new pump, in order to predict its maximum capacity of operation. The objective of a new pump in the experimental unit was to achieve higher flow rates and, consequently, higher Reynolds (Re) ranges.

Figure (10a) shows the graph with the results obtained for pressure drop as a function of the flow rate of water for different layers. Figure (10b) represents the results of the pressure drop as a function of the flow rate of the xanthan gum

solution for different layers in the coiled tubing system.

In Figure (10a), when pumping water, the system reached a maximum flow of 2 m<sup>3</sup> h<sup>-1</sup> reaching the turbulent regime, with a Reynolds value (Re) equal to 1.18×10<sup>4</sup>. In the pumping of xanthan gum, Figure (10b), the system reached a maximum flow of 3 m<sup>3</sup> h<sup>-1</sup>, and, even with a high flow, it did not reach the turbulent regime. The xanthan gum solution reaches higher flow rates because there is a decrease in its viscosity with the increase in shear and, consequently, there is a resistance of the fluid to the flow. This is a characteristic of pseudoplastic fluids such as xanthan gum solutions. The results indicate that changing the pump will enable experiments in flow regions with a higher Reynolds number than currently achieved.

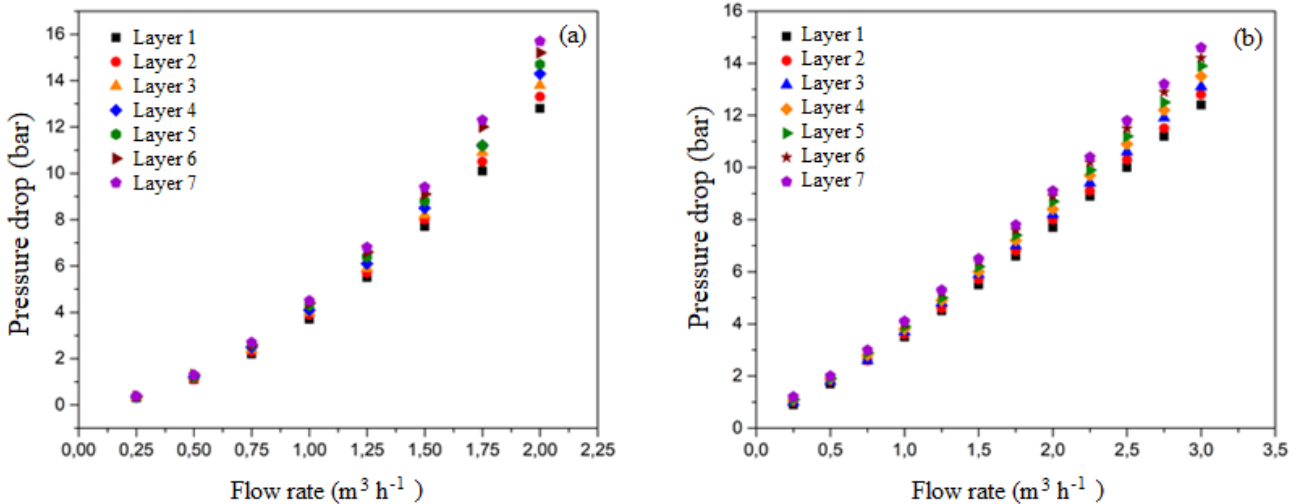


Figure 10 – Experimental data of pressure drop versus flow rate in each layer of (a) water and (b) xanthan gum.

**6. Conclusion**

In the first stage of this work, the case study of the well abandonment process presented, it was possible to observe that the mathematical modeling proposed by Oliveira et al. (2021) was able to predict the pressure drop in the flow of a sequence of Newtonian and non-Newtonian fluids, with an average error relative of 9%. It is important to note that the variation of the curvature ratio in each layer, the variation of the inner diameter in the length of the tube and the pumping of a sequence of fluids were considered.

In the second stage, comparing the values of experimental pressure drops and those predicted by the model proposed by Oliveira et al. (2021), for xanthan gum solutions with a concentration of 0.5

lb bbl-1 and a temperature of 30° and 40°C, it was possible to observe that at 40°C the data had a better fit, with average percentage errors of 18.4%. In relation to the data obtained at a temperature of 30°C, the average percentage errors were 37.8%. It can be concluded that for different flows and temperatures, it is necessary to predict a new friction factor correlation that can better fit the data.

The last part of this study, with experimental tests in the pilot unit, it was possible to predict the maximum flow of operation with a new proposed pump, where the water reached a flow of 2 m<sup>3</sup> h<sup>-1</sup> reaching the turbulent regime (Re = 1.18 x 10<sup>4</sup>), and the xanthan gum reached a maximum operating flow of 3 m<sup>3</sup> h<sup>-1</sup> reaching the laminar regime. The results indicated the need to change

the pump to enable experiments in flow regions with higher Reynolds number, especially for flows of non-Newtonian fluids such as xanthan gum.

## 7. Acknowledgments

Authors would like to thank CENPES (PETROBRAS Research Center) for the support offered for this project development and Scientific support from members of LEF (Laboratório de Escoamento de Fluidos Giulio Massarani).

## References

- Azouz, I., Shah, S.N, Vinod, P.S., and Lord, D.L., 1998. *Experimental Investigation of Frictional Pressure Losses in Coiled Tubing*. SPE Production & Facilities, 13(02), pp. 91–96. doi: 10.2118/37328-PA.
- Bracamonte, J. and Diaz, M., 2018. *No Title*. Available at: <<https://blog.wellcem.com/plug-and-abandonment-coiled-tubing>> [Accessed: 1 November 2021].
- Cioncolini, A. and Santini, L., 2006. *An experimental investigation regarding the laminar to turbulent flow transition in helically coiled pipes*. Experimental Thermal and Fluid Science, 30(4), pp. 367–380. doi: 10.1016/j.expthermflusci.2005.08.005.
- Dean, W. R., 1927. *Note on the motion of Fluid in a Curved Pipe*. Philosophical Magazine and Journal of Science, 20, pp. 208–223.
- ICOTA (Intervention and Coiled Tubing Association) (2019). Available at: <<https://www.icota.com/technical/history>> [Accessed: 1 November 2021].
- Ito, H., 1959. *Friction factors for turbulent flow in curved pipes*. J. Basic Sci. Eng., pp. 123–134.
- Jain, S., Singhal, N. and Shah, S. N., 2004. *Effect of Coiled Tubing Curvature on Friction Pressure Loss of Newtonian and Non-Newtonian Fluids - Experimental and Simulation Study*. All Days. SPE. doi: 10.2118/90558-MS.
- Mashelkar, R. A. and Devarajan, G. V., 1977. *Secondary flows of non-Newtonian fluids: Part III—turbulent flow of viscoelastic fluids in coiled tubes: a theoretical analysis and experimental verification..* Trans. Inst. Chem. Eng., 55, pp. 29–37.
- McCann, R. C. and Islas, C. G., 1996. *Frictional Pressure Loss During Turbulent Flow in Coiled Tubing*. All Days. SPE. doi: 10.2118/36345-MS.
- Medjani, B. and Shah, S. N., 2000. *A new approach for predicting frictional pressure losses of non-newtonian fluids in coiled tubing*. SPE.
- Mishra, P. and Gupta, S. N., 1979. *Momentum Transfer in Curved Pipes. 1. Newtonian Fluids*. Industrial & Engineering Chemistry Process Design and Development, 18(1), pp. 130–137. doi: 10.1021/i260069a017.
- Oliveira, B. R., Leal, B.C., Filho, P.L., Borges, R.F.O., Paraíso, E.C.H., Magalhães, S.C., Rocha, J.M., Calçada, L.A. and Scheid, C.M., 2021. *A model to calculate the pressure loss of Newtonian and non-Newtonian fluids flow in coiled tubing operations*. Journal of Petroleum Science and Engineering. doi: 10.1016/j.petrol.2021.108640.
- Pereira, C. E. G., 2018. *Estudo da perda de carga no escoamento de fluidos Newtonianos em coiled tubing*. Universidade Federal Rural do Rio de Janeiro.
- Shaqilaih, A. and Ahmed Kamel, A., 2013. *AIC Applications in Coiled Tubing Hydraulics*. Proceedings of SPE/IADC Middle East Drilling Technology Conference and Exhibition. Society of Petroleum Engineers. doi: 10.2118/166682-MS.
- Srinivasan, P. S., Nandapurkar, S. S. and Holland, F. A., 1970. *Friction factors for coils*. Trans. Inst. Chem. Eng., 48, pp. T156–T161.
- White, C. M., 1929. *Stream Flow through Curved Pipes*. 51(1903), pp. 645–663.
- White, C. M., 1932. *Fluid friction and its relation to heat transfer*. Trans. Inst. Chem. Eng., 10, pp. 66–86.
- Willingham, J. and Shah, S., 2000. *Friction Pressures of Newtonian and Non-Newtonian Fluids in Straight and Reeled Coiled Tubing*.

Proceedings of SPE/ICoTA Coiled Tubing Roundtable. Society of Petroleum Engineers. doi: 10.2523/60719-MS.

Zhou, Y. and Shah, S. N., 2004. *Rheological Properties and Frictional Pressure Loss of Drilling, Completion, and Stimulation Fluids in Coiled Tubing*. Journal of Fluids Engineering, 126(2), pp. 153–161. doi: 10.1115/1.1669033.